FLASH X-RAY MEASUREMENTS WITH A TIME PROJECTION COMPTON SPECTROMETER

George T. Baldwin, Clinton O. Landron, James R. Lee,

Ramon J. Leeper, and Leonard J. Lorence, Jr.

Sandia National Laboratories

P. O. Box 5800, Albuquerque, NM 87185

SAND--90-0164C

DE90 011050

ABSTRACT

We have developed a "Time Projection Compton Spectrometer" (TPCS) to measure the time-integrated photon energy spectrum between 0.1 and 2 MeV of short-pulse, intense bremsstrahlung sources. A target in the TPCS produces Compton electrons when illuminated by the flash X-ray source. Target electrons are trapped magnetically by current in a rod on the axis of an evacuated drift tube. The curvature and gradient of magnetic field cause the electrons to drift parallel to the spectrometer axis. Time of electron arrival at the end of a 1-m drift encodes the energy spectrum of the X-ray burst. The detector is a plastic scintillator coupled to a fast photomultiplier tube. Despite heavy shielding, enough prompt X rays penetrate to give a time fiducial. Background is measured on shots with the X-ray target removed. The response of the TPCS is calculated using the TIGERP computer code to model photon/electron transport in the target and a sophisticated algorithm to compute electron drift velocity. The response functions and signal are the known components of a matrix equation, which is solved to determine the unknown spectrum. We tested the TPCS with flash X-ray sources on the Saturn accelerator. Signals have been analyzed, spectra unfolded, and results compared with other methods.

Manuscript for submission to

Nuclear Instruments & Methods in Physics Research

(proceedings of the 7th Symposium on

Radiation Measurements and Applications

May 21-24, 1990

The University of Michigan, Ann Arbor, MI)

1. INTRODUCTION

Short-pulse, intense flash X-ray sources are often used for testing the effects of radiation on various electronic components and systems. To understand the mechanisms of the effects properly, it is important to know the energy spectrum of the source.[1] We will limit our consideration to measuring the time integral of the source spectrum. We further restrict our consideration to photon energies between 0.1 and 2 MeV. In some cases, the spectrum can be calculated by computer codes that model coupled electron/photon transport, provided that the voltage and current in the diode of the flash X-ray source are measured accurately. However, diode voltage is often not well known. In certain new diode designs, moreover, the energy of diode electrons is not easily related to the diode voltage.[2] Measuring the photon energy spectrum from sources that are so intense and brief is difficult. Single-particle counting, such as recording pulse heights from a NaI(Tl) or GeLi detector on a multichannel analyzer, is out of the question. Instead, "Compton spectrometers" are a typical solution.[3] In the latter approach, a collimated solid angle of Compton electrons from a thin, low-Z target is dispersed by a steady-state, homogeneous magnetic field. Electrons are sorted by energy according to their differing radii of curvature. X-ray energy follows from the kinematics of the Compton effect.

The "Time Projection Compton Spectrometer" (TPCS), however, uses an entirely different method to determine the energy of the Compton electrons.[4] Figure 1 illustrates the principle of operation. Shown is the drift tube of the spectrometer, which is oriented broadside to the incident photon beam. Electron emission from the target is not collimated. All of the emitted electrons are trapped by the inhomogeneous magnetic field from current in a long straight rod on the axis of the drift tube. The

curvature and gradient of magnetic field cause a net drift of electrons parallel to the spectrometer axis. (See Appendix.) The electrons also spread out in azimuth, but their radial excursion is bounded. A detector some distance from the X-ray target measures electron energy vs. time. The drift velocity of an electron can be related to the energy of the photon that produced it, thus the time evolution of an electron signal encodes the energy spectrum of the flash X-ray burst.

We demonstrated the feasibility of the TPCS in previous experiments [5] on the SPEED flash X-ray machine.[6] The present work describes the results of experiments at the Saturn facility.[7] Several modifications were made to the TPCS, including a custom radiation shield, a different target, and improvements to the collimator, electron detector, and vacuum system. Also, Saturn posed new challenges: a higher-energy X-ray spectrum, a larger-area source, and downward illumination into a basement test cell.

2. DESCRIPTION OF EXPERIMENT

Spectrometer

The current in the center rod of the spectrometer is produced by the discharge of a 2 mF, 100 kJ capacitor bank, connected by four RG-220 coaxial cables to one end of the spectrometer. Negative high voltage goes to the center rod; the case is "ground". A Pearson model 3442 transformer measures the current passing through the center rod. The lumped circuit is about 2.2 μH and 20 mΩ, determined from a ringing waveform at reduced charge. To achieve a peak current of 100 kA, we charge the capacitor bank to 4.75 kV. The current rises in about 90 μs and remains within 1% of peak for about 10 μs, which is comfortably longer than required for the measurement. At peak current, a diode detects voltage reversal and fires an ignitron switch to short the two conductors. This protects the capacitors from voltage oscillation. The current in the TPCS decays exponentially.

We synchronize the X-ray burst with peak current in the TPCS. Saturn takes 3 μs from fire signal to X-ray pulse. The slower capacitor bank must be triggered first. It sends a confirming signal back, which we delay appropriately to fire Saturn.

X rays enter the TPCS through a collimator with a 1.3-cm aperture, as shown in Fig. 2. The collimator has two tungsten elements each 7.6 cm long and separated by 11 cm. The X rays then pass through a Mylar vacuum window, the target, and out through a 9.2-cm-diameter pipe on the opposite side of the drift tube. The center of the beam spot is 5.7 cm from the drift tube axis. The target is polypropylene ($-C_3H_4-$), 12.7 μm thick. Combustion analysis showed 83.2% carbon and 14.5% hydrogen by weight. No high-Z contaminants were revealed by X-ray fluorescence analysis (0.1% threshold; Z>8). Neither technique measures oxygen, which may account for the missing 2.3%. Attached to the side of the X-ray get-lost pipe, a turbomolecular pump evacuates the drift tube below 5×10^{-6} torr to minimize electron energy loss from collisions with air molecules.

At the end of a 1 m drift, electron energy vs. time is measured by the detector shown in Fig. 3. The plastic scintillator is BC-420, which has a 1.3-ns-FWHM response.[8] The face of the scintillator is a ring, 6.7 cm inside- and 16.2 cm outside-diameter, designed to intercept all of the transported Compton electrons. It is 1 cm thick, which is adequate to stop normally-incident 2-MeV electrons. Most actual electron trajectories are oblique, because of the magnetic field. Backscattering is not a problem, because the magnetic field returns scattered electrons to the scintillator. Light emission is therefore proportional to electron energy.[9] The entrant surface of the scintillator is flashed with 200 nm of Al/SiO to improve detector efficiency by reflecting scintillation light. The light passes through a vacuum window and leaves the magnetic field via six pie-shaped,

ultraviolet-transmitting acrylic pipes. A slot for an optional neutral density filter is at the end of the 80-cm light-pipe assembly, immediately in front of the photomultiplier tube (PMT). The PMT is a Hamamatsu model R1250, 5"-diameter, 14-stage, with a bialkali photocathode well-matched to the 390-nm (peak) emission of the scintillator. Bias voltage is -2200 V; gain is 10^6. The voltage divider string is custom-built to optimize the linear output current of the tube. Output is (pulse-)linear to 0.2 A (10 V in 50 Ω), tested with a 100-ns-wide square pulse. The FWHM of the output signal from an impulse illumination measured 4.1 ns. The PMT is encased in conetic and mu-metal sleeves, inside a housing of mild steel, to prevent distortion of tube operation by stray magnetic fields.

The entire TPCS is shielded heavily to reduce the exposure of the detector to source X rays. The case of the shield is formed of 1.2-cm-thick steel and filled (cast) with lead. Overall, the cylindrical shield is 0.9 m diameter, 3.7 m long and weighs more than 20,000 kg. (See Fig. 4.) The cylindrical cavity in the shield is 49 cm diameter and offset from the axis, so that the lead is about 26 cm thick on the side facing the source and 10 cm on the back side. The shield assembles from three modules with overlapped joints. Each module rests on rollers attached to a steel frame. The frame moves on casters. Hydraulic pistons rotate the shield through 90° to point the collimator between horizontal and vertical; the alignment is fixed with turnbuckles. After alignment, lead bricks and shot bags are stacked around the get-lost port to prevent scattered X rays from entering the get-lost opening.

Flash X-Ray Source

We tested the TPCS on the Saturn accelerator. Saturn delivers a 15- to 25-ns-FWHM, 25-TW power pulse to a matched diode load. We expect that peak voltage is between 1 and 2 MV, depending on the diode, but we did not have a

reliable means to measure voltage. Electrons in the diode emerge from concentric cathode rings, are accelerated across a vacuum gap, and stop in tantalum or tungsten-surfaced electrodes. The associated bremsstrahlung emission is concentrated in distinct rings, as revealed by images from an X-ray pinhole camera. A calibrated scintillator/photodiode detector, at approximately the same distance from the source as the TPCS, measured the radiation exposure rate. The intensity varied (again, depending on the diode) by a factor of 5, between 2 and 10 MR/s.

During July 1989, the Saturn radiation source was a bidirectional voltage-dividing (BVD) diode.[2] The area of the source is about 3700 cm^2. In November-December 1989, we tested the TPCS with two other bremsstrahlung diodes. They are smaller: one illuminates a 500 cm^2 irradiation area and the other 3000 cm^2.[10] For the latter two diodes, the diode voltage is higher, which poses a more difficult radiation background problem for the TPCS.

The TPCS target in all cases was 5.4 m from the diode center, and off axis by 34°. The (elliptical) field of view was about 220 cm^2. We aligned the TPCS with the center of the 500 cm^2 diode. For the BVD and 3000 cm^2 diodes, the collimator pointed off to one side of the center such that all emitting rings were sampled. Alignment was done by sighting from behind the get-lost port through the collimator apertures.

3. ANALYSIS

The response of the TPCS is calculated by Monte Carlo methods using TIGERP, a one-dimensional coupled electron/photon transport code.[11] The response is determined for X-ray distributions that are uniform over specified intervals of photon energy. The calculations use the dimensions and elemental composition of the TPCS target to model the production, scattering, and energy loss of electrons during their escape from the

target. We assume that photons are normally incident and neglect the effect of the magnetic field on electron trajectories within the foil. Given the velocity vector of an emitted electron, a sophisticated algorithm computes the collisionless-drift time-of-flight per unit length, for a specified rod current.[12] We assume that all electron energy is deposited in the scintillator (electron energy is unchanged during the drift) and the detector response is linear with energy. The computer code assembles a response function by tabulating electron energy as a function of drift time.

We correct these impulse response functions to account for the finite time response of the detector, which is dominated by the 4-ns-FWHM PMT response. Detector response affects all X-ray energies equally. We also must consider that the electrons are not produced instantaneously by an X-ray pulse with a finite duration. However, the source duration is not the same for all X-ray energies, because the voltage changes during the pulse. High-energy X rays have a relatively short duration; low-energy X rays persist with a longer duration. The pulse width correction is very small at high energy and has little effect on the response at low-energy. Figure 5 is a plot of the 18 response functions for a 12.7-μm-thick polypropylene target and 100 kA center rod current, broadened with a 4-ns-FWHM triangular function. We used these to unfold the spectrum from TPCS signals taken with the BVD diode on Saturn.

The calculated response functions $F_i(t)$ and measured signal $S(t)$ are the known components of an integral equation, which is here approximated by a summation over discrete energy bins, ΔE_i:

$$S(t) \approx \sum_{i=1}^{M} F_i(t) \cdot N_i \cdot \Delta E_i \qquad (1)$$

N_i are the relative numbers of photons in each bin of the differential energy spectrum. The unknown coefficients, $N_i \Delta E_i$, are determined by minimizing the square of the difference between the actual signal and its approximation, integrated over an appropriate time span:

$$\frac{\partial}{\partial(N_j \Delta E_j)} \left\{ \int_t \frac{1}{\sigma^2(t)} \left[S(t) - \sum_{i=1}^{M} F_i(t) \cdot N_i \cdot \Delta E_i \right]^2 dt \right\} = 0 \qquad (2)$$

We assume that the error in the signal, $\sigma(t)$, does not change with time. Taking the derivatives gives M equations in M unknowns:

$$\int_t S(t) \cdot F_j(t) \cdot dt = \sum_{i=1}^{M} N_i \cdot \Delta E_i \cdot \int_t F_i(t) \cdot F_j(t) \cdot dt \qquad j=1 \ldots M \qquad (3)$$

which is solved by matrix methods to determine the unknown spectrum. The solver is a routine from a mathematical library that forces a non-negativity constraint and factors the matrix by elimination with symmetric pivoting.[13] To check the solution, we compare the result of the least squares fit, i.e., the summation in equation (1) above, with S(t). The individual terms of the summation are the "weighted response functions," which indicate the relative contribution of each spectral bin to the overall TPCS signal.

4. RESULTS

Figure 6 shows the TPCS signals from four shots with the BVD diode. The traces have been shifted to align the peak of the prompt pulse with t=0. The amplitudes are scaled to overlay the prompt pulses. Three shots had a target. A 0.6 neutral density filter attenuated the scintillator emission by a factor of 4 to bring the signal within the linear range of the PMT. Shot #733 was a background shot with both the target foil and the neutral density filter removed, otherwise identical to the target shots. The non-

zero background following the prompt signal is approximately a factor of 18 less than the electron signals from the target shots.

The prompt component of the signal on all four shots is the response of the electron detector to the X-ray burst. Some X rays penetrate the shield; others scatter from the region of the collimator, target, and get-lost pipe. The prompt signal indicates when the drifting electrons left the target (t=0). The target-out background shot is subtracted from each target shot before unfolding the spectrum.

Figure 7 shows the unfolded spectra corresponding to the three target shots in Fig. 6. Figure 8 is the reconstructed signal for shot 732, which compares the spectrum unfold solution with the background-corrected TPCS signal.

During the November-December Saturn run with the 500 cm^2 and 3000 cm^2 diodes, we studied the radiation background problems associated with these higher-voltage sources. There are four important test results:

(1) We were able to increase the amplitude of the delayed (electron) peak relative to the amplitude of the prompt (X-ray) peak by using a wider target. Figure 9 shows at least a threefold improvement by using a target sufficiently wide to intercept most of the beam spot from the collimator.

(2) By lowering the bias on the PMT from -2200V to -1500V, the delayed/prompt peak amplitude ratio was further enhanced. As shown in Figure 10, shot 801, at -2200V bias, shows a 6:1 prompt- to delayed-amplitude ratio. Shot 806, at -1500V, has improved to a 1:2 ratio.

(3) The X-ray background in the prompt peak is at least partly due to the inherent response of the PMT, seen by comparing shots 801 and 802 in Fig. 10. The prompt pulse is substantial despite black cloth covering the PMT.

(4) The effect of the target holder on the delayed electron background is not appreciable, as shown in Fig. 11. Nevertheless, the holder is kept in place for target-out shots.

5. DISCUSSION

"Time projection" of Compton electrons has a significant advantage over "spatial projection" (i.e., with spectrometers that use a homogeneous magnetic field), because the signal is time-separated from prompt X-ray background. Also, the signal is maximized, because the TPCS accepts all electrons from the target, not just a narrowly-collimated fraction of the emission.

An important feature of the TPCS is the single electron detector. Only one data acquisition channel is required. Energy "channels" are defined by partitioning the signal in time; they are not fixed by the hardware design of the spectrometer. The chance for systematic errors between different "channels" is reduced.

For comparison, a differential absorption spectrometer (DAS) was fielded on the BVD diode shots. The DAS is a stack of thermoluminescent dosimeters (TLDs) between various thicknesses of various materials, which filter the spectrum.[14] Figure 12 compares the spectra determined by the TPCS and DAS. The TPCS reveals that higher-energy X rays are present than in the DAS unfold. This is not too surprising, because the response functions for TLD filtration all become flat (spectrally insensitive) at higher energies. The DAS unfold is severely underdetermined, with only 13 TLDs used to adjust a 30-bin spectrum. The iterative solution therefore depends strongly on an accurate trial spectrum. In contrast, the TPCS unfold makes no a priori assumptions about spectral shape.

There are several important improvements that could be made to the TPCS:

A higher center-rod current and/or a longer drift would improve the separation between prompt background and electron signal, which is most important for spectrum measurements with the higher-voltage diodes. Energy resolution also improves. In this experiment, attempts to exceed 100 kA in the center rod produced unpredictably-large background from arcs at current contacts. Hardware modifications can solve the problem for future tests.

The appreciable sensitivity of the PMT alone limits our ability to adjust detector sensitivity with neutral density filters. A lower-gain PMT is preferable. We accomplished this by lowering the PMT voltage; in so doing, linear output current was sacrificed. A PMT specially designed for lower gain, yet high linear current, is desirable. Also, we need to measure detector efficiency.

Although the increased ratio of prompt to electron signals at higher voltage was compensated with a larger illuminated target, there are limits. The pitch of the helical path of the guiding center for low-energy electrons is small. Low-energy electrons might intercept the target again if it becomes too wide. Likewise, the energy of slow electrons would be distorted if the target were thicker.

Comprehensive analysis of errors and their propagation through the unfolding algorithm needs to be studied. We have represented the spectrum as a histogram for simplicity, but there may be more appropriate basis functions. Also, the "joints" between spectral bins might be better chosen to improve the condition of the unfold matrix.

6. CONCLUSION

We have measured the X-ray energy spectrum from a Saturn flash X-ray source using a Time Projection Compton Spectrometer. Results were compared with a differential absorption spectrometer. Tests at higher voltages confirmed ways to compensate for increased radiation background. Higher

current in the spectrometer and a lower-gain detector would be significant improvements. Such development would exploit the potential advantages of the TPCS, particularly for measuring the spectrum from higher-energy sources.

7. APPENDIX

An extensive analysis of electron drift velocity in a 1/r magnetic field is given in Reference 12. An approximate formula for the drift velocity, v_d, accurate in the high-field limit (ε large), is:

$$v_d \approx \frac{v}{2\varepsilon}\left[\, 1 + \xi^2 \,\right]$$

where:

$$\varepsilon \equiv \frac{2eI}{mc^3\gamma\beta} \approx 0.117\,\frac{I}{\gamma\beta}\,, \quad I \text{ in kA}$$

is a dimensionless field parameter, and:

$$\xi \equiv \left(\frac{v_\phi}{v}\right) e^{v_z/\varepsilon v}$$

is a constant of the motion. γ, β are the relativistic parameters for the electron. v_ϕ and v_z are the azimuthal and axial components of the instantaneous electron velocity, v. For the broadside illumination of the TPCS target, forward-peaked Compton emission gives $v_\phi \approx v$, $\xi \approx 1$ and $v_d \approx v/\varepsilon$. The TPCS is essentially a "compressed" time-of-flight method, where the instantaneous electron velocity is reduced by the factor ε. For 100 kA, ε is about 6.8 at 0.511 MeV and 4.1 at 1.02 MeV.

8. ACKNOWLEDGMENTS

Measurements were performed while collaborating on a number of experiments to develop new diode designs for the Saturn flash X-ray facility. These experiments were directed by Victor Harper-Slaboszewicz, Mark Hedemann and Arthur Sharpe. We much appreciate the assistance of the

Saturn operations, control/monitor and data acquisition staff in fielding the experiment, particularly Brad Peyton, Robin Broyles, Kevin Berry, Dave Tanner, Bob Ross and Blake Henderson. Analysis of the TPCS targets was performed by Karen Higgins, Pam Puissant and Leif Singman. Abbe Mattson and others at EG&G Las Vegas did the assembly and characterization of the PMT. Ken Shimp and Kent Shelton assisted with the engineering design of the radiation shield. We thank Victor Harper-Slaboszewicz for reviewing the paper. Research is funded by the Department of Energy under contract no. DE-AC04-76DP00789.

FIGURE CAPTIONS

Fig. 1. Schematic of the Time Projection Compton Spectrometer. The TPCS captures all electrons from the target. The radius of the Larmor orbit of the electron varies with distance from the center rod. Consequently, the electron has a net axial drift, which depends on the electron energy. (Note: the helical path of the guiding center is not to be confused with the much-tighter Larmor orbit of the electron.)

Fig. 2. Illumination geometry of the TPCS X-ray target. The X-ray beam passes through a two-element tungsten collimator, a 12.7-μm-thick polypropylene foil, and out through a get-lost port. The drift tube is evacuated through the get-lost port.

Fig. 3. Electron detector. Drifting electrons stop in the plastic scintillator, BC-420. 200-nm-thick aluminumized flashing on the scintillator surface improves light collection efficiency. Six light pipes carry the scintillator signal out of the high-current region to a fast, 10^6-gain phototube that is well shielded from magnetic fields. Each light pipe is a 60° sector that tapers to pass through the spokes of the current return plate.

Fig. 4. Photograph of the TPCS assembled in its X-ray shield in the Saturn exposure cell. The X-ray source is out of the picture, above right. The capacitor bank is in the background. Shield plugs for access ports and lead-brick assembly around get-lost port are not shown. The elevator is down and safety cage pulled back during a shot.

Fig. 5. Response functions used to unfold X-ray energy spectrum. The X-ray energy bins are spaced non-uniformly, as indicated in the legend. The response functions assume an 12.7-μm-thick

polypropylene target, 100 kA center-rod current, 1 m drift, and 4-ns-FWHM time response of the electron detector. Dashed- and dotted-line curves are scaled up by factors of 10 and 100, respectively, for readability.

Fig. 6. Signals from four shots with the bidirectional voltage-dividing (BVD) diode on Saturn. Shot 733 was a background shot with the TPCS X-ray target removed. The other three shots used a 12.7-μm-thick polypropylene target. Center rod current was 100 kA on all four shots. The amplitudes have been scaled as shown to overlay the prompt peaks.

Fig. 7. X-ray spectrum unfold results for the three BVD diode target shots on Saturn, from Fig. 6.

Fig. 8. Reconstructed signal for shot 732. The dotted curves are the response functions from Fig. 5, each weighted by the corresponding value of the spectrum from Fig. 7. The sum of these "weighted response functions" is the dashed curve, which approximates the recorded TPCS signal (solid curve).

Fig. 9. Effect of increased target width. The target in shot 791 was much narrower than the beam spot size. In shot 799, the target width was six times wider. (The area of the beam spot on the target was about four times greater).

Fig. 10. Radiation background due to inherent PMT response. Shots 801 and 802 were the same except that the neutral density filter in 801 was replaced by black cloth in 802. Shots 801 and 806 both had finite neutral density filters (801-2, 806-1.2), but the PMT gain on 806 was dropped by lowering the bias voltage from -2200V to -1500V. Shot 806 has been scaled (× ND-0.8) to compensate for the different ND filters.

Fig. 11. Effect of target holder. Neither shot 810 nor 811 used a target. Shot 810 left the Lexan foil holder in place; in 811, it was removed. Shot 811 is scaled to match the prompt peak amplitude in 810.

Fig. 12. Comparison of TPCS and DAS results for BVD diode X-ray spectrum (3 shots). The TPCS unfold is plotted as a histogram; the DAS unfold is a line plot. The spectra are normalized to the same value at the 316 keV point in the DAS spectrum.

REFERENCES

1] V. A. J. van Lint, Mechanisms of Radiation Effects in Electronic Materials, Vol. 1, Wiley-Interscience, 1980; simulation fidelity studies by W. Beezhold and others at Sandia National Laboratories.

2] V. J. Harper-Slaboszewicz, J. R. Lee, M. A. Hedemann, G. T. Baldwin, J. W. Poukey, L. J. Lorence, Jr., G. A. Carlson, W. E. Fowler, D. L. Faucett, and C. O. Landron, "Operation of a bidirectional voltage-dividing bremsstrahlung diode," J. Appl. Phys., 67(7),3233 (Apr. 1990).

3] J. W. Motz, William Miller, H. O. Wyckoff, H. F. Gibson, and F. S. Kirn, "Gamma-Ray Measurements by the Magnetic Analysis of Compton Electrons," Rev. Sci. Instr., 24, 929 (October 1953).

4] G. T. Baldwin and J. R. Lee, "Time Projection Compton Spectrometer," IEEE Trans. Nucl. Science, NS-33(6), 1298 (December 1986).

5] G. T. Baldwin, C. O. Landron, J. R. Lee and R. J. Leeper, "Experimental Demonstration of a Time Projection Compton Spectrometer," Bull. Amer. Phys. Soc., 33(9), 1948 (October 1988).

6] J. F. Seamen, J. P. VanDevender, D. L. Johnson, T. H. Martin, G. Zawadzkas, E. L. Neau, W. Beezhold, K. Mikkelson, S. Downie, and D. Green, "SPEED, a 2.5 TW, Low Impedance Pulsed Power Research Facility, Proc. of the 4th IEEE Pulsed Power Conference (Albuquerque, NM), M. F. Rose and T. H. Martin, ed., 68 (June 1983).

7] D. D. Bloomquist, R. W. Stinnett, D. H. McDaniel, J. R. Lee, A. W. Sharpe, J. A. Halbleib, L. G. Schlitt, P. W. Spence, and P. Corcoran, Proc. of the 6th IEEE Pulsed Power Conference (Arlington, VA), P. J. Turchi and B. H. Bernstein, ed., 310 (June 1987)

8] Bicron Corporation, Newbury, Ohio, BC-420 data sheet (Feb. 1987).

9] E. Brannen and G. L. Olde, "The Response of Organic Scintillators to Electron Energy Deposited in Them," Radiation Research, 16, 1 (1962).

10] M. A. Hedemann, private communication, 1989.

11] J. A. Halbleib, Sr., and J. E. Morel, "TIGERP," (Computer Code Abstract), Nucl. Sci. & Eng., 70, 213 (1979).

12] J. R. Lee, "Techniques for Calculating the Drift Velocity of an Electron Moving in a 1/r Magnetic Field," SAND89-0241, Sandia National Laboratories report (March 1989).

13] K. H. Haskell and R. J. Hanson, "An Algorithm for Linear Least Squares Problems with Equality and Nonnegativity Constraints," Math. Programming, 21(1), 98 (July 1981).

14] G. A. Carlson and L. J. Lorence, "A Differential Absorption Spectrometer for Determining Flash X-ray Spectra from 10 to 2000 keV," IEEE Trans. Nucl. Sci., NS-35(6), 1255 (December 1988).

Fig. 1

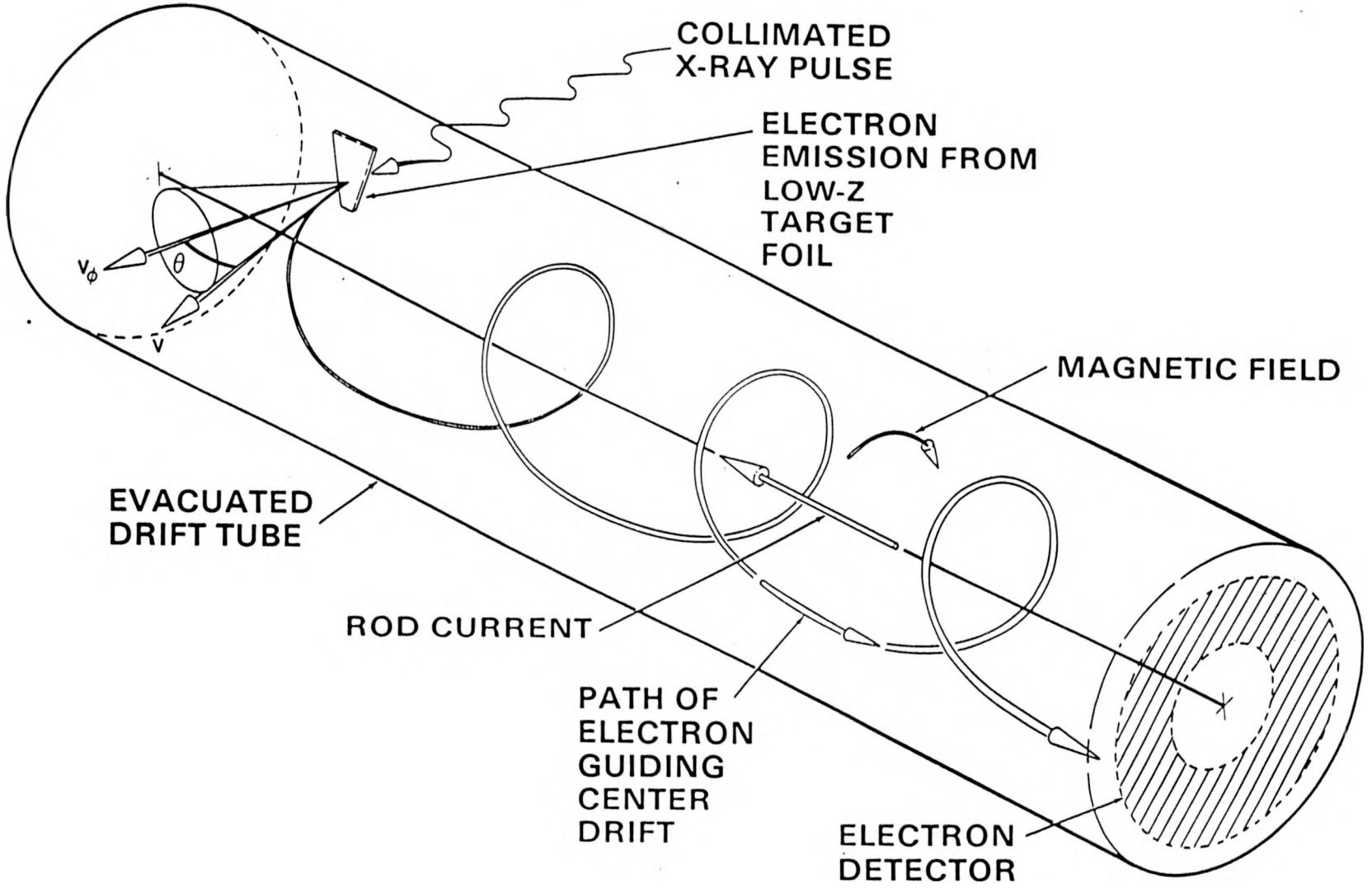
COLLIMATED
X-RAY PULSE
ELECTRON
EMISSION FROM
LOW-Z
TARGET
FOIL
v_ϕ
θ
v
MAGNETIC FIELD
EVACUATED
DRIFT TUBE
ROD CURRENT
PATH OF
ELECTRON
GUIDING
CENTER
DRIFT
ELECTRON
DETECTOR

Fig. 2

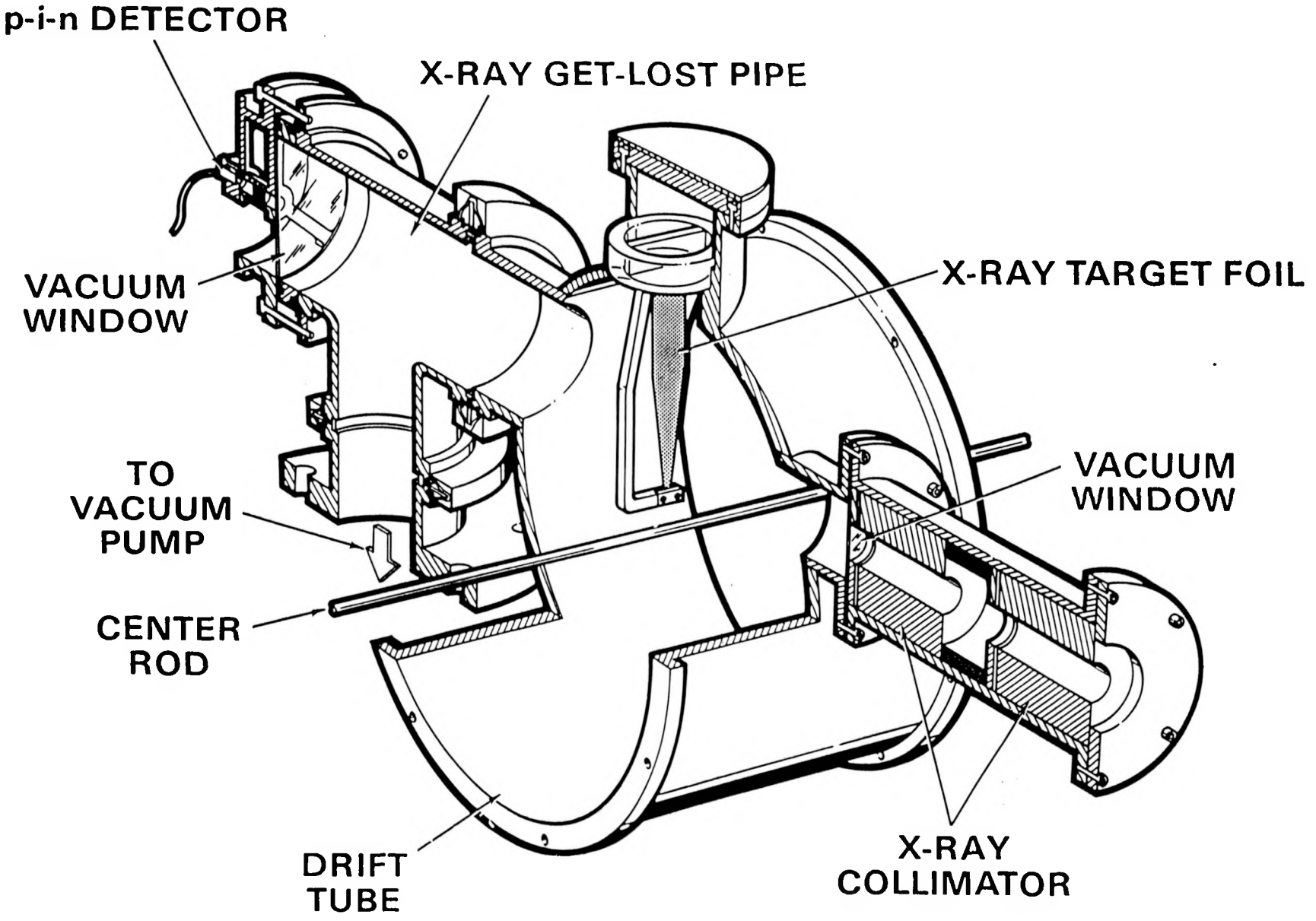
p-i-n DETECTOR
X-RAY GET-LOST PIPE
VACUUM WINDOW
X-RAY TARGET FOIL
TO VACUUM PUMP
VACUUM WINDOW
CENTER ROD
DRIFT TUBE
X-RAY COLLIMATOR

Fig. 3

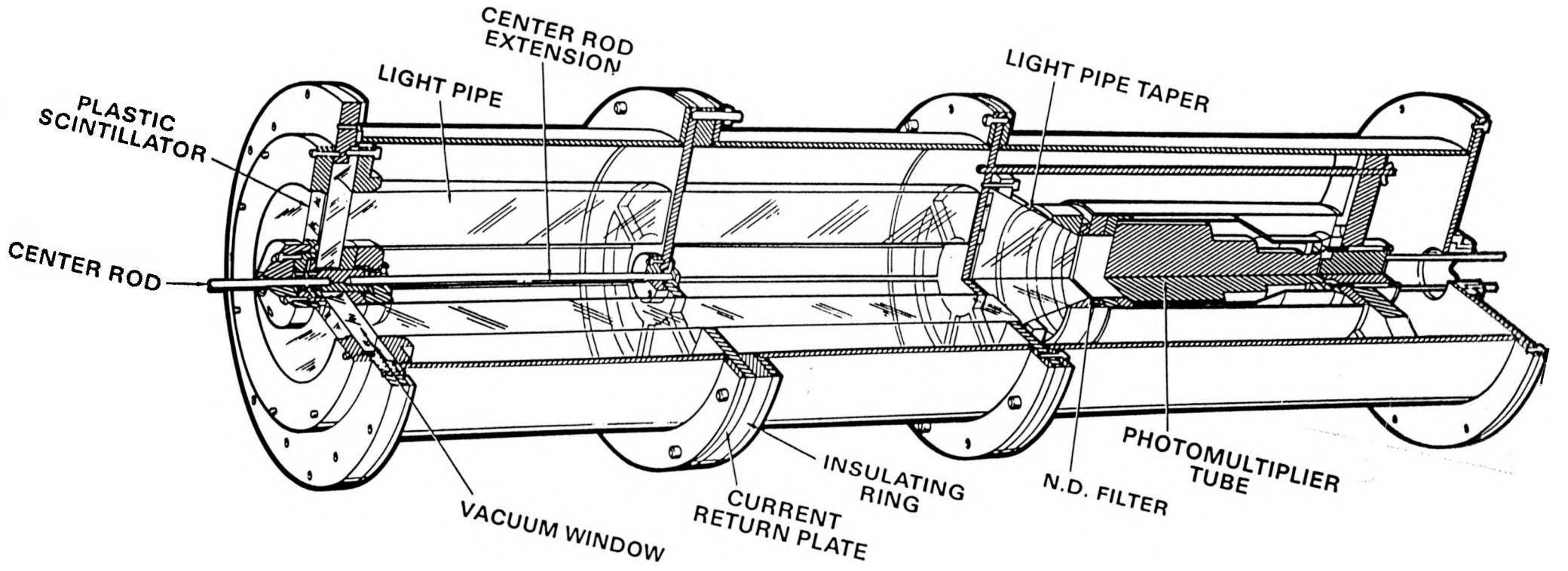
CENTER ROD EXTENSION
LIGHT PIPE
LIGHT PIPE TAPER
PLASTIC SCINTILLATOR
CENTER ROD
VACUUM WINDOW
CURRENT RETURN PLATE
INSULATING RING
N.D. FILTER
PHOTOMULTIPLIER TUBE

Fig. 4

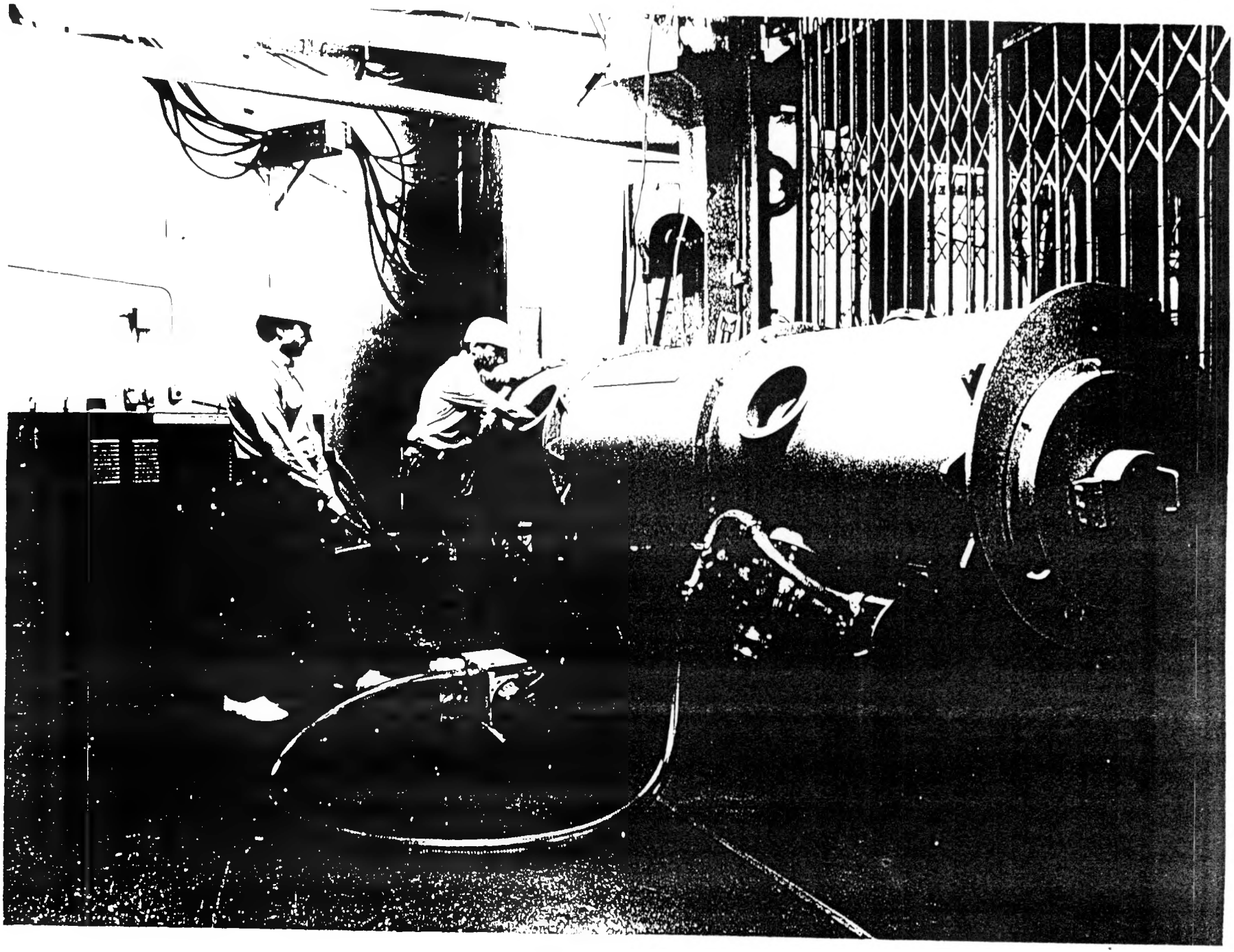

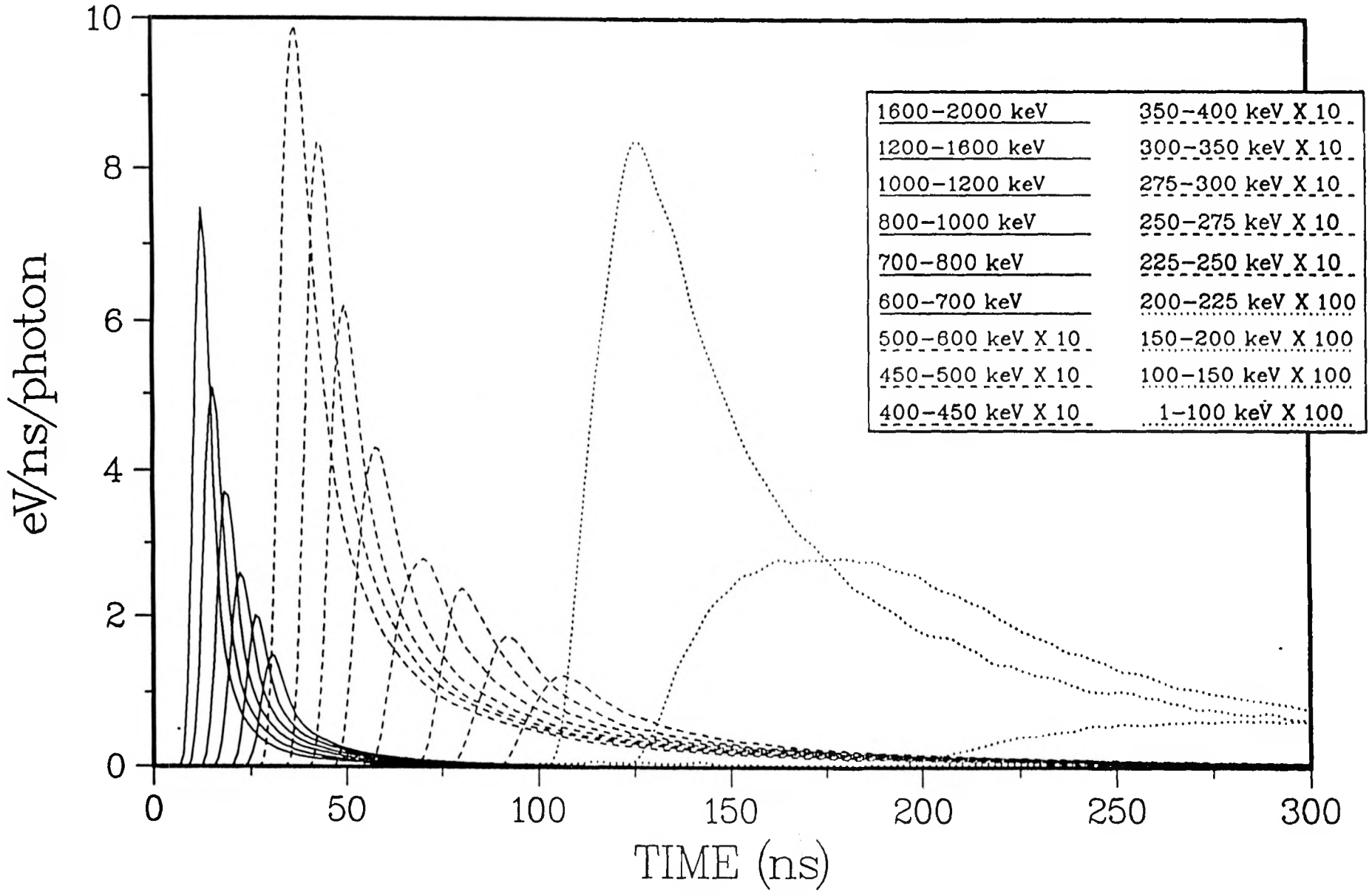
10
8
6
4
2
0
eV/ns/photon
0
50
100
150
200
250
300
TIME (ns)
1600–2000 keV
1200–1600 keV
1000–1200 keV
800–1000 keV
700–800 keV
600–700 keV
500–600 keV X 10
450–500 keV X 10
400–450 keV X 10
350–400 keV X 10
300–350 keV X 10
275–300 keV X 10
250–275 keV X 10
225–250 keV X 10
200–225 keV X 100
150–200 keV X 100
100–150 keV X 100
1–100 keV X 100

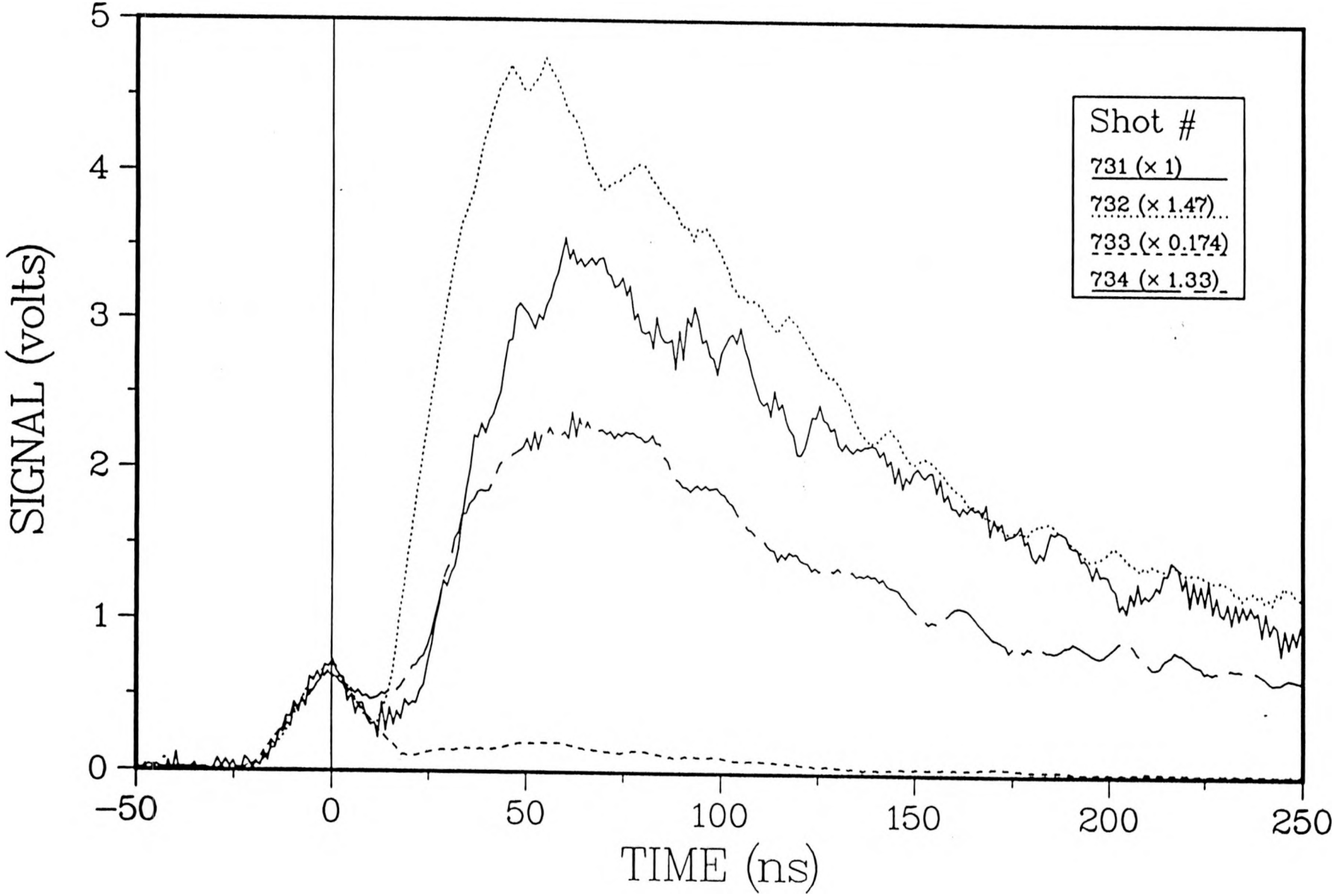
Shot #
731 (× 1)
732 (× 1.47)
733 (× 0.174)
734 (× 1.33)
SIGNAL (volts)
TIME (ns)
0
1
2
3
4
5
−50
0
50
100
150
200
250

Fig. 7

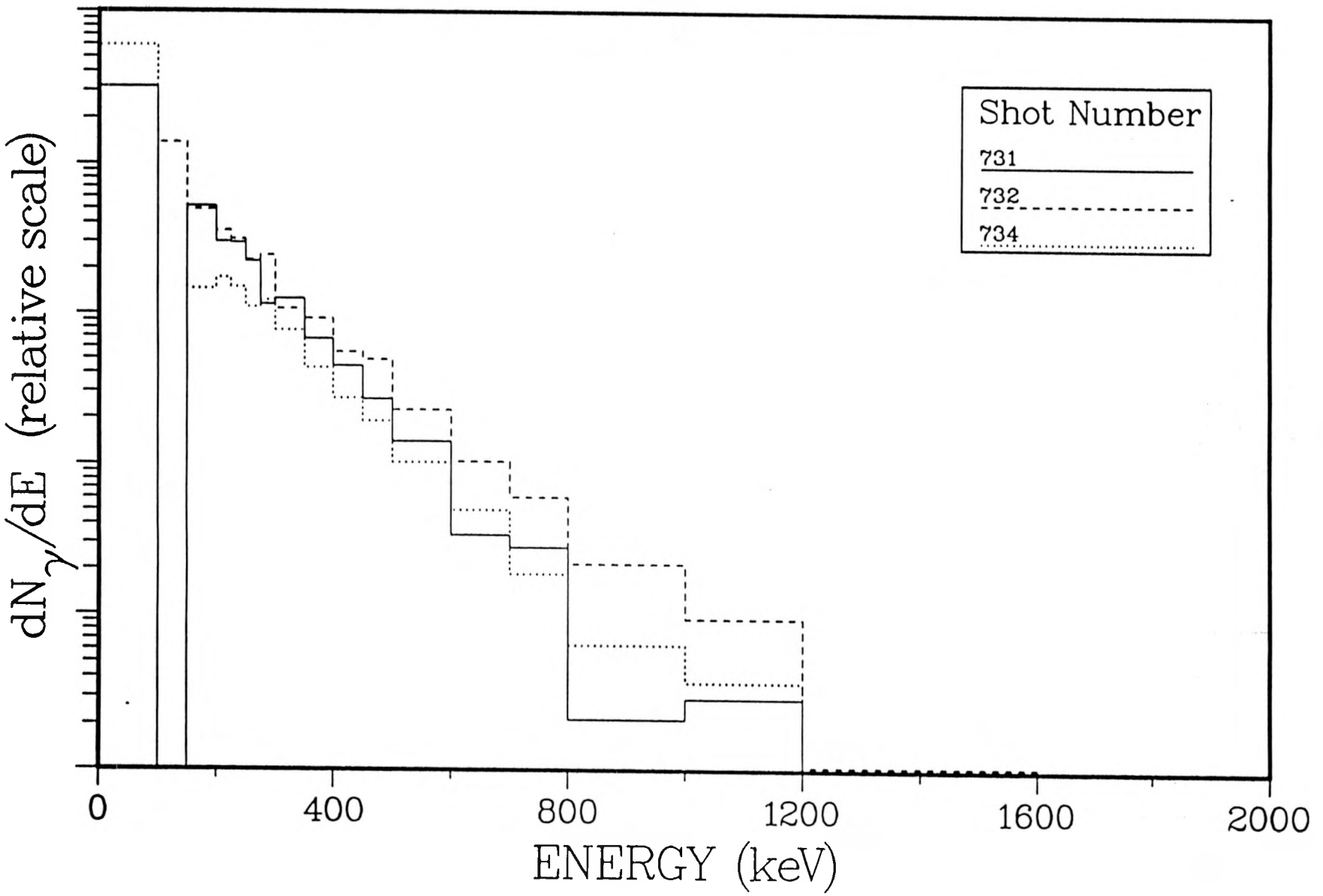
Shot Number
731
732
734
dN$_\gamma$/dE (relative scale)
0
400
800
1200
1600
2000
ENERGY (keV)

Fig. 8

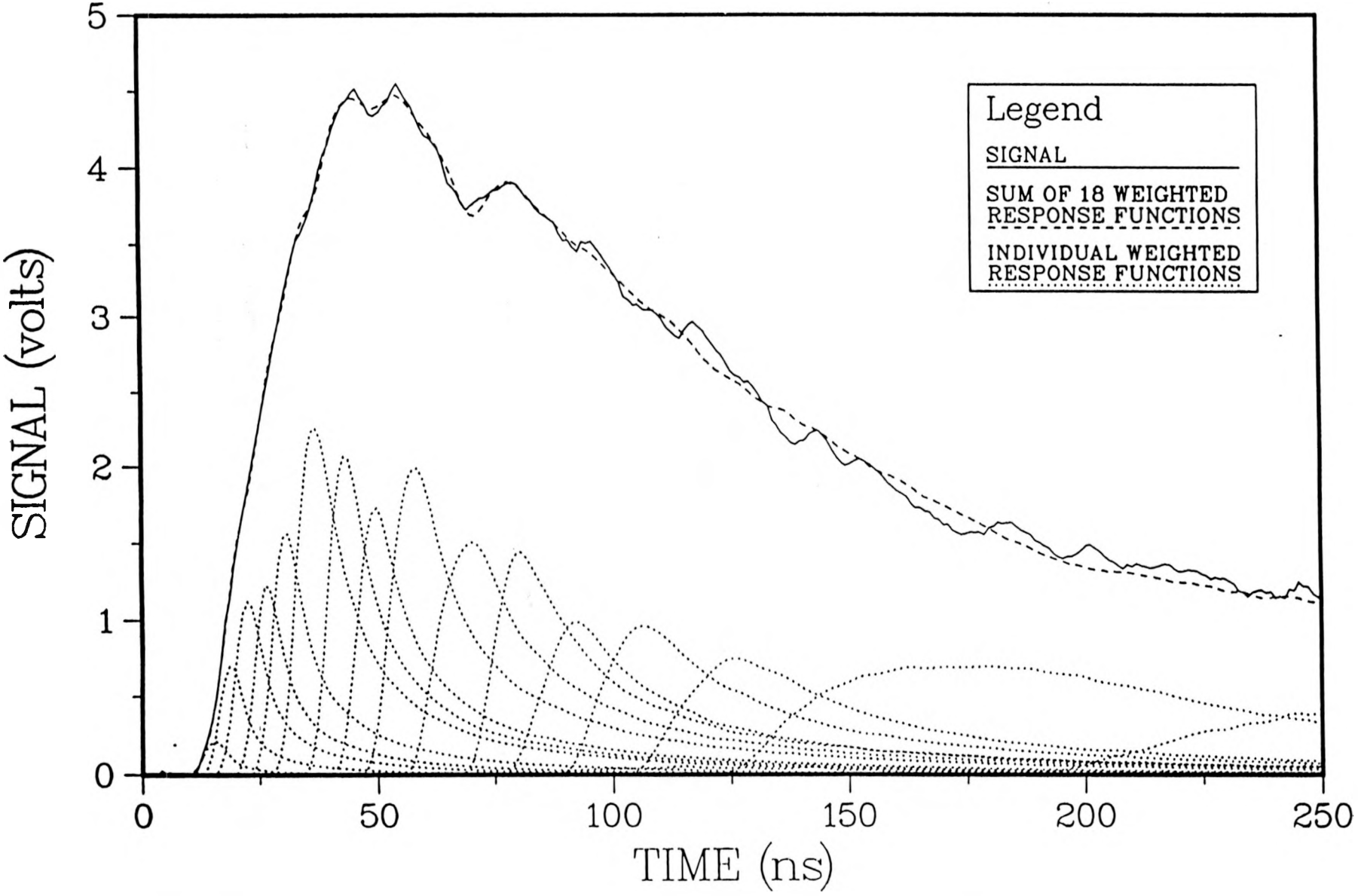
Legend
SIGNAL
SUM OF 18 WEIGHTED RESPONSE FUNCTIONS
INDIVIDUAL WEIGHTED RESPONSE FUNCTIONS
SIGNAL (volts)
TIME (ns)
0
1
2
3
4
5
0
50
100
150
200
250

Fig. 7

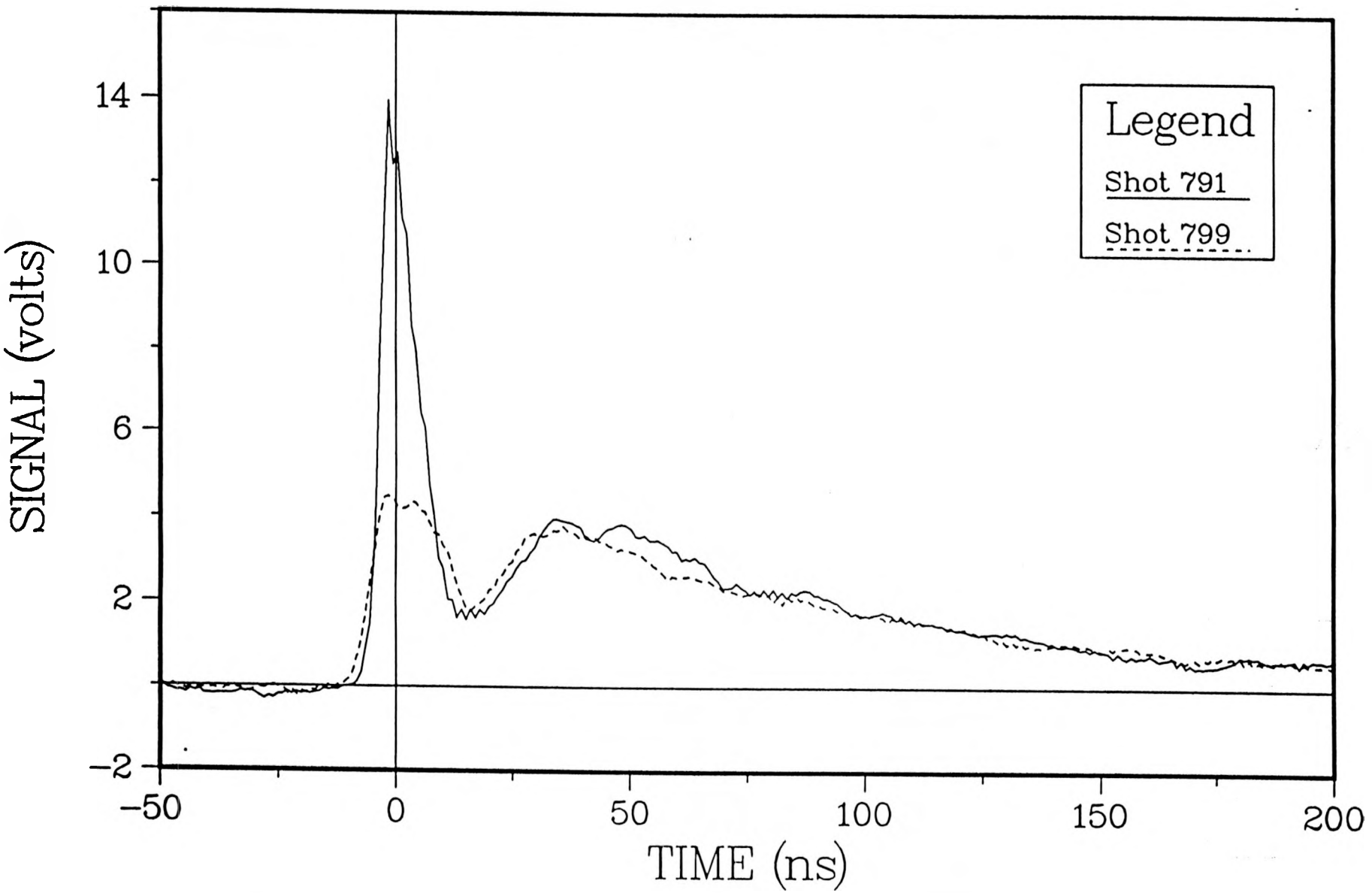
Legend
Shot 791
Shot 799
SIGNAL (volts)
14
10
6
2
−2
−50
0
50
100
150
200
TIME (ns)

Fig. 10

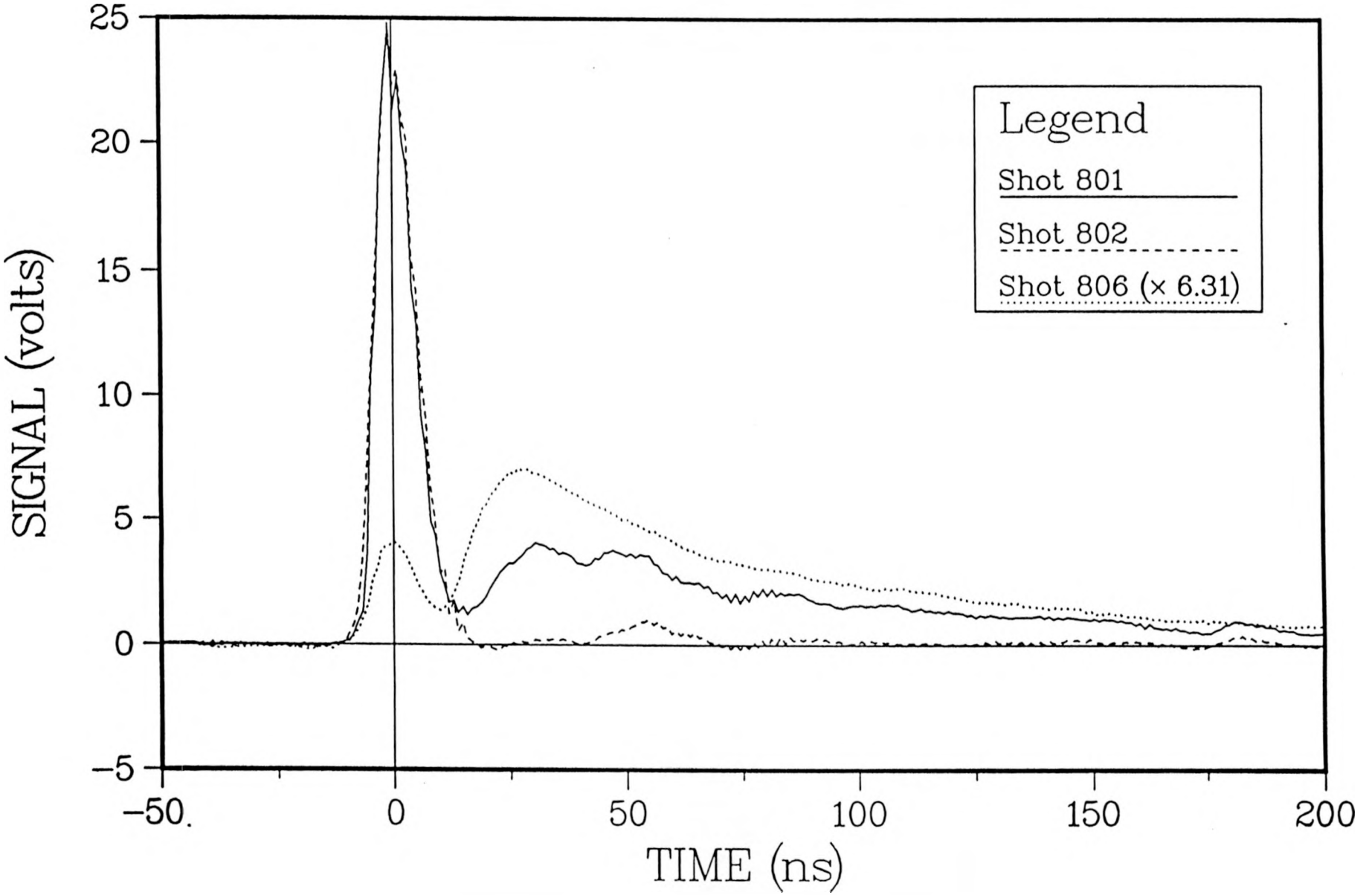
Legend
Shot 801
Shot 802
Shot 806 (× 6.31)
SIGNAL (volts)
25
20
15
10
5
0
−5
−50.
0
50
100
150
200
TIME (ns)

Fig. 11

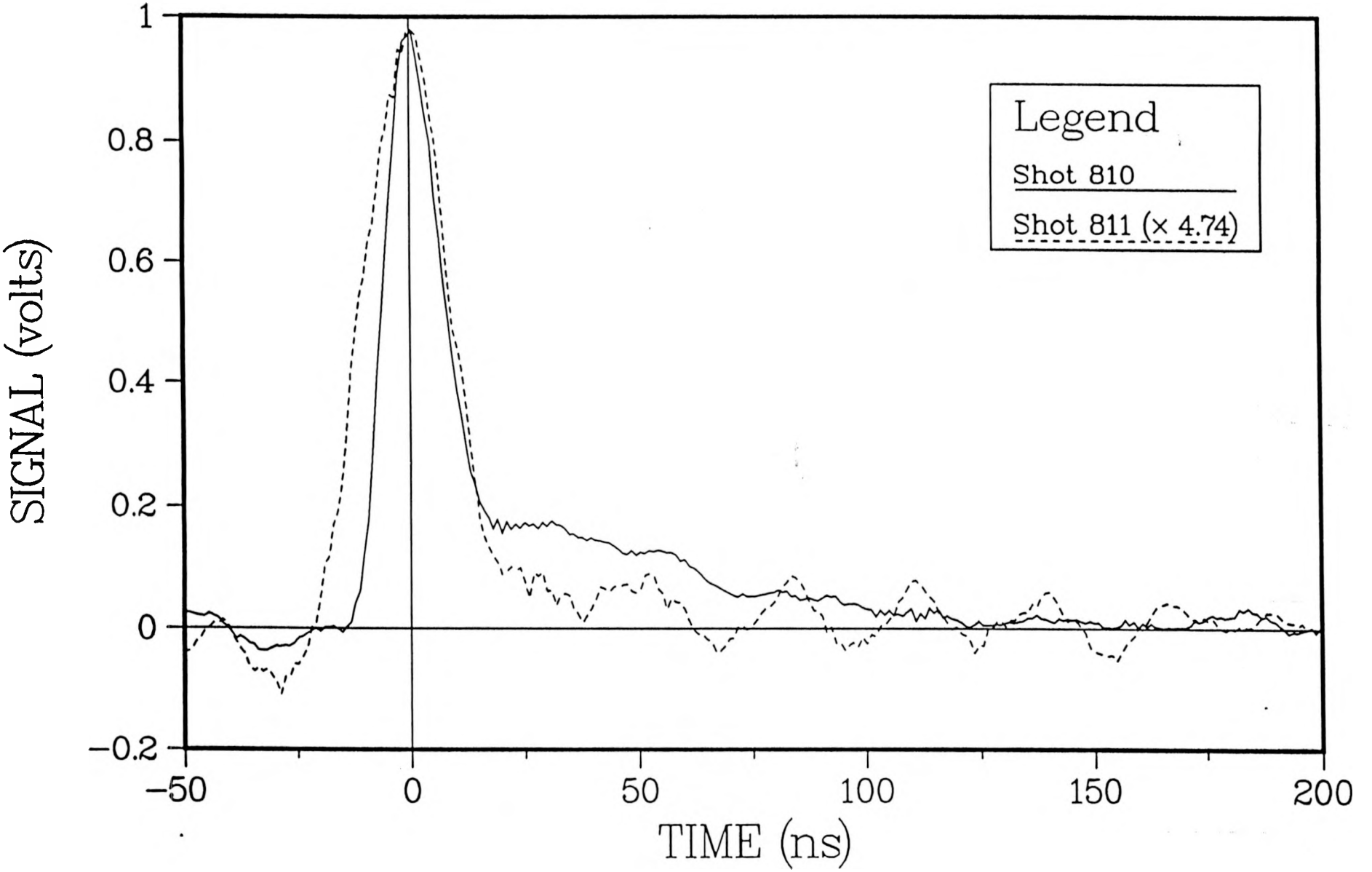
Legend
Shot 810
Shot 811 (× 4.74)
SIGNAL (volts)
1
0.8
0.6
0.4
0.2
0
−0.2
−50
0
50
100
150
200
TIME (ns)

Fig. 12

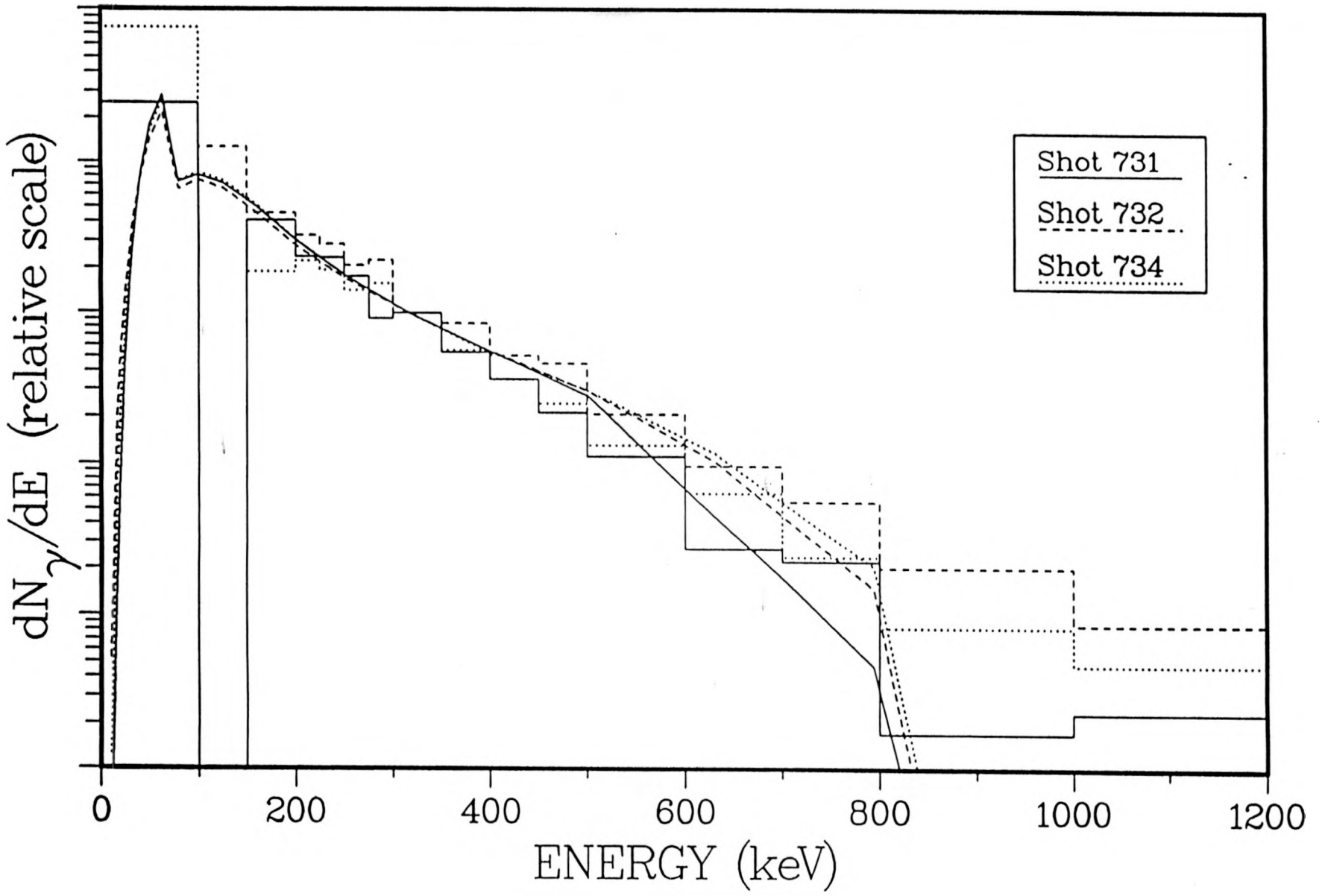
Shot 731
Shot 732
Shot 734
dN$_\gamma$/dE (relative scale)
0
200
400
600
800
1000
1200
ENERGY (keV)